The Lymphocyte Function–associated Antigen 1 I Domain Is a Transient Binding Module for Intercellular Adhesion Molecule (ICAM)-1 and ICAM-3 in Hydrodynamic Flow

By Ruth Knorr and Michael L. Dustin

From the Center for Immmunology and Department of Pathology, Washington University School of Medicine, St. Louis, MO 63110

Summary

The I domain of lymphocyte function–associated antigen (LFA)-1 contains an intercellular adhesion molecule (ICAM)-1 and ICAM-3 binding site, but the relationship of this site to regulated adhesion is unknown. To study the adhesive properties of the LFA-1 I domain, we stably expressed a GPI-anchored form of this I domain (I-GPI) on the surface of baby hamster kidney cells. I-GPI cells bound soluble ICAM-1 (sICAM-1) with a low avidity and affinity. Flow cell experiments demonstrated a specific rolling interaction of I-GPI cells on bilayers containing purified full length ICAM-1 or ICAM-3. The LFA-1 activating antibody MEM-83, or its Fab fragment, decreased the rolling velocity of I-GPI cells on ICAM-1–containing membranes. In contrast, the interaction of I-GPI cells with ICAM-3 was blocked by MEM-83. Rolling of I-GPI cells was dependent on the presence of Mg^{2+}. Mn^{2+} only partially substituted for Mg^{2+}, giving rise to a small fraction of rolling cells and increased rolling velocity. This suggests that the I domain acts as a transient, Mg^{2+}-dependent binding module that cooperates with another Mn^{2+}-stimulated site in LFA-1 to give rise to the stable interaction of intact LFA-1 with ICAM-1.

Regulated adhesion is crucial for a fast and flexible immune response (1–3). After leukocyte activation, lymphocyte function–associated antigen 1 (LFA-1)[1] is rapidly converted from inactive (low avidity) to active (high avidity) with respect to binding to intercellular adhesion molecule 1 (ICAM-1). This increase in avidity results in adhesion strengthening and can be regulated either from the inside or the outside of the cell. Factors regulating LFA-1 affinity from the outside of the cell include natural ligands under in vivo conditions and activating antibodies, the divalent cation Mn^{2+} or EGTA treatment in the presence of excess Mg^{2+} under in vitro conditions (3). It also has been reported that immunoaffinity purification of LFA-1 in the presence of Mg^{2+}, but not Ca^{2+} (1) resulted in an increase in the affinity for ICAM-1. The structural changes in LFA-1 leading to adhesion strengthening are not known.

One approach to understanding the structural basis of LFA-1 affinity regulation is to study ligand binding properties in LFA-1 subdomains. Although there have been several reports indicating ligand binding sites in different subdomains in LFA-1 (4, 5), the best characterized is a 200 amino acid inserted domain (I domain) in the LFA-1 α subunit (6–10). The I domain has sequence similarity to diverse proteins that are involved in adhesion and is also present in the α subunit of a subset of integrins. Mapping studies with monoclonal antibodies using immunofluorescence and cell adhesion in Mac-1 and p150,95 subunit chimeras (11), as well as homotypic aggregation and ICAM-1 binding to T cells (12), indicated both function blocking and activating epitopes in the I domain. Furthermore, these studies suggested a possible interaction of the Mac-1 I domain with iC3b, fibrinogen, and ICAM-1 (11), and of the LFA-1 I domain with ICAM-1 and ICAM-3 (12). Also, a soluble dimeric LFA-1 I domain-Fc fusion protein was shown to bind to ICAM-1–coated surfaces in ELISA assay, but it lacked the characteristic divalent cation dependence of the LFA-1/ICAM-1 interaction (6). This was in contrast to soluble forms of the Mac-1 A domain, which bound to the Mac-1 ligands iC3b (13), ICAM-1, and fibrinogen (14) in a cation-dependent manner. Further experiments using human/murine (7, 10) and human/chicken (15) chimeras of the LFA-1 and VLA-1 I

[1]*Abbreviations used in this paper:* BHK, baby hamster kidney; I-GPI, GPI anchored form of the LFA-1 I domain; ICAM, intercellular adhesion molecule; LFA, lymphocyte function–associated antigen; PIPLC, phosphatidylinositol-specific phospholipase C.

Portions of this work were previously presented at the meeting of the American Association for Immunologists (AAI) on 3-6 June 1996 in New Orleans, LA.

domain, respectively, extended the initial mapping studies and showed binding of the LFA-1 I domain to ICAM-1 and the VLA-1 I domain to laminin and collagen IV. By site-directed mutagenesis, ligand binding residues in the I domain of LFA-1 (7, 9, 10), Mac-1 (9), VLA-1 (15), and VLA-2 (9) were defined. Evidence for a functional role of these residues was also obtained from the crystal structure of the Mac-1 A domain, which revealed a novel metal-ion–dependent adhesion site with the coordinating motif DxSxS (16). Up to date, the crystal structures of the Mac-1 A domain in the presence of Mg^{2+} (16) and Mn^{2+}(17) and the LFA-1 I domain in the presence of Mn^{2+} (18), Mg^{2+}, and EDTA (19) have been determined. The domain adopts a fold of alternating α-helices/β-sheets, called Rossman fold.

In this study, we analyzed the interaction of the I domain with ICAMs in the context of cell adhesion using laminar flow adhesion assays. The flow cell system has been used in a variety of approaches to study transient, selectin-, or integrin-mediated interactions, as well as stable attachments. This system is suitable to measure quantitatively interactions with high dissociation rates (~1 to ~8 s^{-1}; references 20 and 21, respectively), consistent with estimates obtained by surface plasmon resonance. In contrast with surface plasmon resonance, the flow cell system allows analysis of transient interaction between surface-attached proteins and their purified ligands reconstituted in planar bilayers, yielding avidities and rolling velocities, which are related to the affinities and off-rates, respectively. The accuracy reached with the flow cell is in the range of atomic force microscopy (21), thereby rendering the flow cell technology a useful complement to other techniques. Our results show that the I domain of LFA-1 supports rolling adhesion in flow, but does not mediate stable adhesion. Therefore, we propose that the I domain has binding properties similar to selectins in conferring a transient, strain-resistant binding to full length purified ICAM-1 and ICAM-3. Furthermore, our results show that the I domain is more active in the presence of Mg^{2+} than Mn^{2+}. Together these data suggest that there is another Mn^{2+}-stimulated ligand binding site in the intact LFA-1 molecule, which cooperates with the I domain to account for the stable interaction between high affinity LFA-1 and ICAMs.

Materials and Methods

Cell Lines and Antibodies. The T-lymphoma line SKW3 was obtained from T. Springer (Center for Blood Research, Boston, MA) and baby hamster kidney (BHK)/VP16 from T. Warren (Monsanto Chemical Co., St. Louis, MO) (22). MEM-83 was a gift from V. Horesji (Institute of Genetics, Videnska, Czech Republic). ICR3 was donated by D. Staunton (ICOS Corp., Bothell, WA), CL203 by S. Ferrone (New York Medical College, Valhalla, NY), RR1/1 and sICAM-1 by R. Rothlein (Boehringer Ingelheim, Ridgefield, CT). TS1/22 and TS2/9 were from the American Type Culture Collection (Rockville, MD).

Recombinant DNA. CD2 cDNA was obtained from C. Hession (Biogen, Inc., Cambridge, MA), the cDNA of the α-chain of LFA-1 from D. Griggs (Monsanto Chemical Co.) and the Decay Accelerating Factor–based GPI-anchoring vector from D. Lublin (Washington University, St. Louis, MO) (23).

Generation of the Membrane-anchored I Domain Constructs. A GPI-anchored I domain (I-GPI) was generated by overlap extension PCR (24). Two parallel PCR reactions used LFA-1α cDNA as template (Fig. 1 *A*). In reaction 1, the signal peptide coding segment was ligated to an 18-bp linker derived from the 5′ end of repeat II in the LFA-1α cDNA. In reaction 2, the I domain (V130-S327) was generated with a 33-bp linker derived from the 5′ end of repeat III in the LFA-1α cDNA. Overlap between primers 2 and 3 was used to join the signal peptide/linker fragment to the I domain fragment in a final PCR. Primer 4 contains a HindIII site that was used to subclone the product of the final PCR in frame into a GPI anchoring vector (23).

To generate I-EF, a ClaI site in the coding region of the I domain was used. A ClaI-EcoRI fragment comprising part of the coding region for the I domain and the GPI anchoring signal was replaced with the 912-bp fragment comprising part of the coding region for the I domain, repeat III, IV, V, VI, and 30 bp of repeat VII of the LFA-1 α-chain. I-CD2 contained the coding regions of the original I domain linked to a few basepairs at the 3′ end of domain 1, the coding sequences for the linker region, domain 2, and the stalk of CD2. To generate I-CD2, the HindIII site in I-GPI was treated with Klenow fragment and ligated blunt end to the SspI site in the coding region of CD2. To allow the removal of the whole coding region of domain 2 of CD2, an XbaI site was engineered at the joint between the coding region of domain 2 and the transmembrane domain. I-EF and I-CD2 were linked in frame to the GPI anchoring signal as in I-GPI (23). I-GPI was subcloned into pMON3360B (Monsanto Chemical Co.) and stably transfected into BHK/VP16 cells with lipofectamine (22). I-GPI, I-EF, and I-CD2 subcloned into pCDNA3 (Invitrogen, San Diego, CA) were used for transient transfection in COS-1 cells (25).

Flow Cytometry and Generation of Fab Fragments. Clones were tested for surface expression of I-GPI, I-EF, and I-CD2 with TS1/22 and MEM-83 by immunofluorescence flow cytometry on a FACScan® (Becton Dickinson & Co., Mountain View, CA). MEM-83 and TS1/22 Fab fragments were generated by incubating 200 μg of monomeric IgG with papain agarose (0.74 U) in the presence of 20 mM cystein for 1 h at 37°C (26). The reaction was terminated by addition of excess iodoacetamide. Absence of intact IgG was confirmed by electrophoresis of 10 μg of the Fab on SDS-10%-PAGE minigel followed by silver staining (detection limit <10 ng).

Phosphatidylinositol-specific Phospholipase C Treatment and Western Blotting. ~10^6 washed BHK cells were incubated for 60 min at 37°C in 100 μl Hanks buffered salt solution (HBSS), 2 mM Hepes with 0.1, 0.2, or 0.6 U phosphatidylinositol-specific phospholipase C (PIPLC; 13.3 U/ml; ICN, Costa Mesa, CA) in HBSS, 2 mM Hepes, and 1 mg/ml ovalbumin, respectively. Cells were pelleted by centrifugation at 800 *g* for 10 min. The proteins contained in supernatant and pellet were separated by SDS-PAGE under reducing conditions (12% Tris/Glycine gel) and transferred to nitrocellulose by electroblotting. Western blotting was carried out according to the description of the manufacturer (ECL; Amersham Corp., Cleveland, OH). TS1/22 (10 μg/ml) was used as primary antibody.

Purification of Adhesion Molecules. Full-length ICAM-1, ICAM-3, LFA-1, and LFA-3 were purified from cell lysates by immunoaffinity chromatography as described previously (27). Briefly, JY cell lysate (ICAM-1, LFA-1, and LFA-3) or SKW3 cell lysate

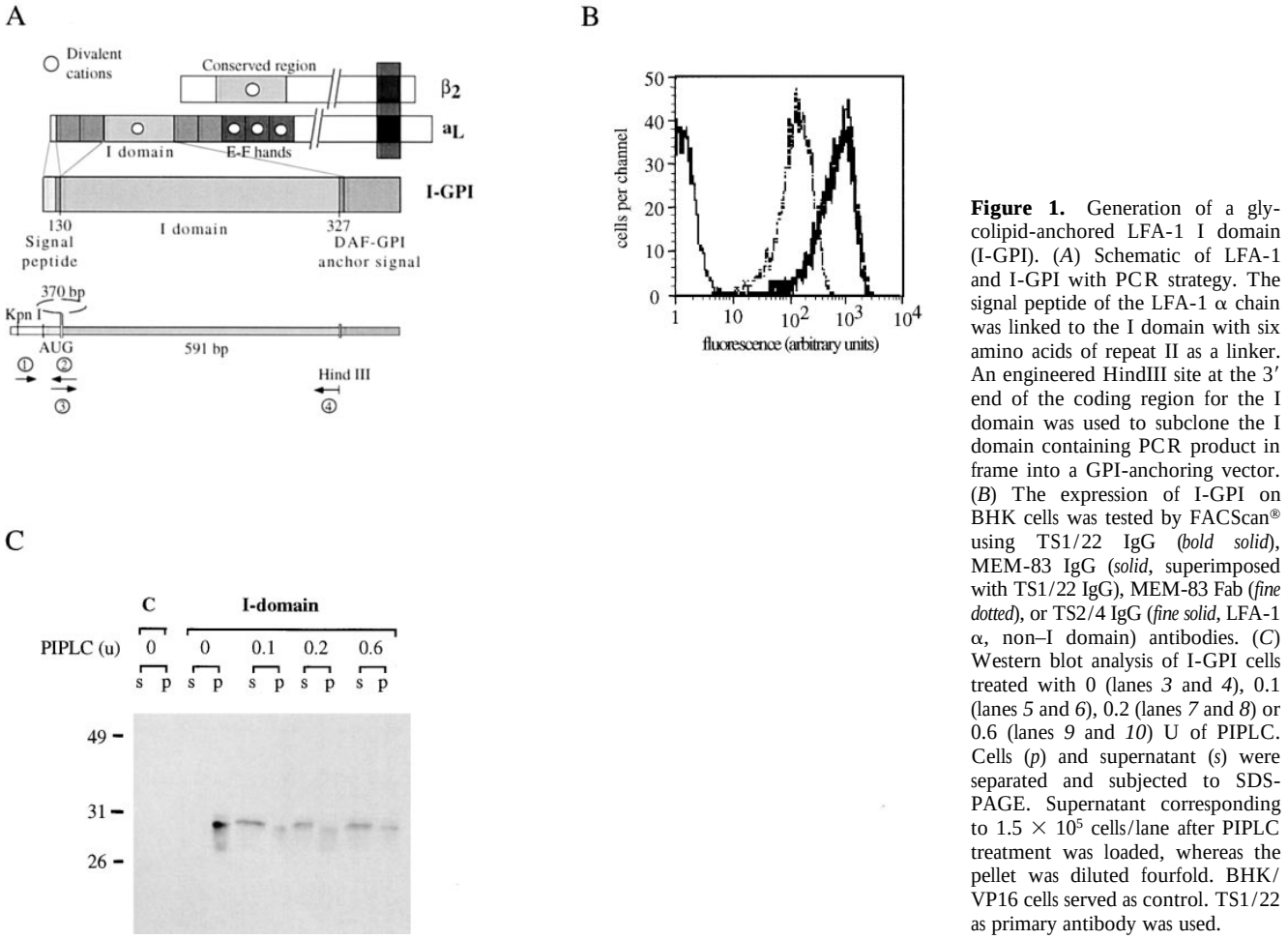

Figure 1. Generation of a glycolipid-anchored LFA-1 I domain (I-GPI). (*A*) Schematic of LFA-1 and I-GPI with PCR strategy. The signal peptide of the LFA-1 α chain was linked to the I domain with six amino acids of repeat II as a linker. An engineered HindIII site at the 3′ end of the coding region for the I domain was used to subclone the I domain containing PCR product in frame into a GPI-anchoring vector. (*B*) The expression of I-GPI on BHK cells was tested by FACScan® using TS1/22 IgG (*bold solid*), MEM-83 IgG (*solid*, superimposed with TS1/22 IgG), MEM-83 Fab (*fine dotted*), or TS2/4 IgG (*fine solid*, LFA-1 α, non–I domain) antibodies. (*C*) Western blot analysis of I-GPI cells treated with 0 (lanes *3* and *4*), 0.1 (lanes *5* and *6*), 0.2 (lanes *7* and *8*) or 0.6 (lanes *9* and *10*) U of PIPLC. Cells (*p*) and supernatant (*s*) were separated and subjected to SDS-PAGE. Supernatant corresponding to 1.5×10^5 cells/lane after PIPLC treatment was loaded, whereas the pellet was diluted fourfold. BHK/VP16 cells served as control. TS1/22 as primary antibody was used.

(ICAM-3) were passed sequentially over a bovine IgG precolumn, and a CL203 (ICAM-1), TS2/4 (LFA-1), TS2/9 (LFA-3), or ICR3 (ICAM-3) column. ICAM-1 was eluted at pH 12.5 and LFA-1, LFA-3, and ICAM-3 were eluted at pH 3.5. The proteins were quantified by immunoradiometric assay using RR1/1, ICR3, TS1/22, and TS2/9 antibodies. The purity of the proteins was confirmed by SDS-PAGE and silver staining of the gels. The purified proteins were incorporated into egg L-α-phosphatidylcholine (Egg-PC; Avanti Polar Lipids, Alabaster, AL) by detergent dialysis (28).

Competitive Binding Assay with Radiolabeled Fab Fragments. TS1/22 Fab fragments were iodinated to a specific activity of 15 μCi/μg. The dissociation constant (K_d) for the TS1/22 Fab binding to I-GPI E6 cells was 10 nM. 2×10^4 I-GPI E6 cells were preincubated with 10–200 μM soluble ICAM-1 (sICAM-1) and 2 nM TS1/22 Fab fragments. The binding of the TS1/22 Fab fragments was terminated after 20 min by centrifugation (4,500 rpm, 3 min; room temperature) through a 100-μl oil cushion containing 60% dibutyl- and 40% dioctyl-phthalate in microsedimentation tubes (72.702; Sarstedt, Inc., Newton, NC). Cell pellet and supernatant were separated by cutting off the lower part of the tubes. The K_d for the interaction of the I domain and ICAM-1 was determined by using the formula of Cheng and Prusoff (29): $K_d^{ICAM\text{-}1} = IC_{50}/(1 + ([Fab]/K_d^{Fab}))$, whereby IC_{50} represents the concentration of sICAM-1 necessary for 50% inhibition of iodinated Fab-fragment binding; [Fab] represents the concentration of iodinated Fab fragments and K_d^{Fab} is the K_d for binding of the Fab fragments to I-GPI.

Static Cell Adhesion Assays. Purified ICAM-1 was absorbed to polystyrene microtiter plates (Corning Medical and Scientific, Cambridge, MA) as described (30) and prewashed with assay medium shortly before use. SKW3 and I-GPI cells were fluorescently labeled by incubation with calcein-AM (C-3100; Molecular Probes, Eugene, OR; 1 μg/ml calcein-AM in RPMI-1640, 2% BSA; 37°C, 45 min, 5% CO_2) or BCECF-AM (B-1170; Molecular Probes; 10 μg/ml BCECF in DME, 2% FBS; 37°C, 60 min, 10% CO_2), respectively. Labeled SKW3 cells were stimulated with phorbol 12-myristate-13-acetate (PMA; Sigma Chemical Co., St. Louis, MO; 50 ng/ml) for 15 min. 2×10^5 fluorescently labeled cells in 100 μl RPMI-1640, 2% BSA were distributed per well and the adhesion determined as described recently (27). All points were determined as quadruplicates and averaged.

Adhesion in Hydrodynamic Flow. Adherent BHK cells were suspended by incubation with Hank's balanced salt solution/20 mM Hepes/5% FBS/0.5 mM EDTA, washed with 20 mM Hepes, pH 7.4, 137 mM NaCl, 2.3 mM KCl, 1% BSA (HBS/BSA) containing the indicated divalent cations at 2 mM $MgCl_2$ or EDTA, 1 mM $CaCl_2$, or 0.2 mM $MnCl_2$, and resuspended at $1–2 \times 10^6$ cells/ml. When indicated, cells were incubated with antibodies at 100 μg/ml IgG or 10 μg/ml Fab for 60 min at 4°C in HBS/BSA and the appropriate divalent cation, washed, and subjected onto planar bilayer membranes. Purified ICAM-1, ICAM-3, LFA-1, or

LFA-3 was reconstituted into unilamellar Egg-PC liposomes such that the planar bilayers formed from the liposome suspensions contained 500 sites/μm^2 (ICAM-1, LFA-1, or LFA-3) or 1,000 sites/μm^2 (ICAM-3) as determined by immunoradiometric assay (31). The planar bilayers were formed on a glass coverslip that was mounted in a parallel plate flow cell (Bioptechs, Butler, PA) with a 250-μm gap between the coverslips. Cells were visualized on an inverted microscope (Yona Microscopes, Silver Spring, MD) using a 10× objective with bright-field optics. Images were recorded on an S-VHS video cassette recorder (Panasonic, Secaucus, NJ). The cells were allowed to settle on the planar bilayer surface for 2 min without flow, and then subjected to increasing shear stresses from 1.1–21.3 dyn/cm^2, doubling the flow rate every 30 s with a syringe pump (Harvard Apparatus, Inc., South Natick, MA). The velocity of rolling cells was reduced at least 100-fold compared with free cells at 1.1 dyn/cm^2. All flow cell experiments were done at 18–20°C. Percent cells free, rolling, or attached was determined by counting cells in the initial static field, and then starting flow at 1.1 dyn/cm^2 (1 ml/min) and counting cells at 29 s after start of flow. Data are means of two to seven experiments in which ~100 cells were initially present per field. The rolling velocity was determined by digitizing 16–17 images spanning 23 s at low flow rates or 17 s at high flow rates from S-VHS tape and measuring the distance individual cells moved in the given timeframe. 20–50 individual cells derived from different experiments were analyzed.

Results

Adhesion of a GPI-anchored Form of the LFA-1 I Domain to ICAM-1 is Similar in Affinity and Avidity to Adhesion of Unstimulated T Cells. To address the adhesive function of the LFA-1 I domain, a GPI-anchored form of the I domain was designed by overlap extension PCR (24) (Fig. 1 *A*) and stably expressed in BHK cells. Clones were tested for surface expression of the I domain by immunofluorescence analysis (FACScan®) using the antibodies TS1/22 and MEM-83, both of which bind to the LFA-1 I domain (7, 12) (Fig. 1 *B*). The presence of a GPI anchor was assessed by treatment of I-GPI cells with PIPLC (32). Release of an expected 30-kD soluble I domain into the supernatant was detected by Western blotting using TS1/22 antibody (Fig. 1 *C*). For subsequent studies, clones were selected expressing 10^6 (I-GPI E6) and 10^5 (I-GPI E5) GPI-anchored I domain molecules per cell, as determined by I^{125} TS1/22 binding.

In initial experiments to determine the affinity of the I domain, the binding of radiolabeled sICAM-1 dimers to I-GPI E6 cells was not detectable (data not shown). Subsequently, we measured the inhibition of binding of radiolabeled TS1/22 Fab fragments to I-GPI E6 cells by titrating in sICAM-1 (Fig. 2 *A*). Half maximal reduction of TS1/22 Fab binding was achieved at ~150 μM sICAM-1. Using the formula of Chen and Prusoff (29), the K_d for the I domain/ICAM-1 interaction was calculated to be in the range of 100–200 μM, as determined in three independent experiments. This result indicates that the affinity between sICAM-1 and the I domain is low and similar to the affinity of sICAM-1 and intact LFA-1 on unstimulated T cells (~100 μM) (33).

Next, we tested the ability of I-GPI cells to adhere to purified ICAM-1 in a plate binding assay (Fig. 2 *B*). As shown previously (30), half-maximal binding of PMA-stimulated SKW3 cells, which express LFA-1 in the high avidity state, was observed at 150 ICAM-1 molecules/μm^2. In the absence of PMA, 5000 ICAM-1 molecules/μm^2 were necessary to detect half-maximal binding of unstimulated SKW3 cells. I-GPI E5 cells expressed a number of I-GPI molecules, which corresponds to the number of LFA-1 molecules expressed on activated T cells. I-GPI E5 cells (Fig. 2 *B*) did not adhere to ICAM-1–coated surfaces, even at site densities up to 5,000 molecules ICAM-1/μm^2. I-GPI E6 (Fig. 2 *B*), expressing the I domain at a superphysiological level at 10^6 molecules/cell, reached 50% binding to ICAM-1–coated plates at a site density of 5,000 molecules/μm^2. Apparently, very high levels of I-GPI and very high ICAM-1 site densities are required to form sufficient bonds for "stable" adhesion. We conclude from these experiments that the interaction between the LFA-1 I domain and ICAM-1 is in a similar range as unstimulated SKW3 cells and of low avidity.

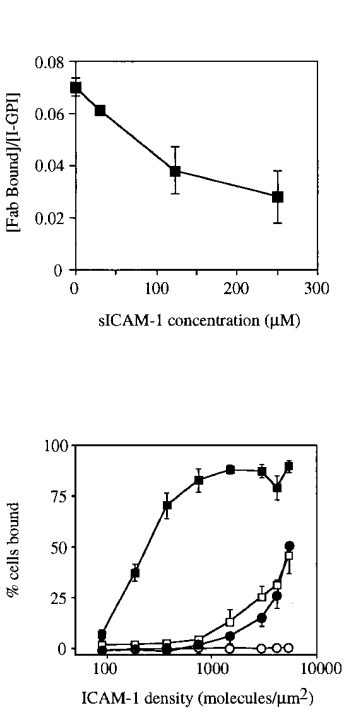

Figure 2. Competition of sICAM-1 with ^{125}I TS1/22 Fab fragments for binding to I-GPI (*A*) and static adhesion assay of SKW3 cells and I-GPI cells to ICAM-1 coated on plates (*B*). (*A*) I-GPI E6 cells were incubated with the indicated concentrations of sICAM-1 and ^{125}I TS1/22 Fab fragments (2 nM) for 20 min at room temperature. Cells and supernatant were separated by centrifugation through an oil cushion. The binding of TS1/22 Fab fragments is expressed as a fraction of I domain sites. Protein concentration in the assay was kept constant with ovalbumin. The result represents one experiment out of three. (*B*) Unstimulated SKW3 cells (*open squares*), SKW3 cells preincubated with 50 ng/ml PMA (*filled squares*), and I-GPI E6 cells (*closed circles*) or I-GPI E5 cells (*open circles*) were tested for adhesion to ICAM-1–coated plastic at 37°C in RPMI-1640, 2% BSA. Purified ICAM-1 was coated on polystyrene at the indicated density as determined by immunometric assay. SKW3 cells were labeled with calcein AM and BHK cells with BCECF.

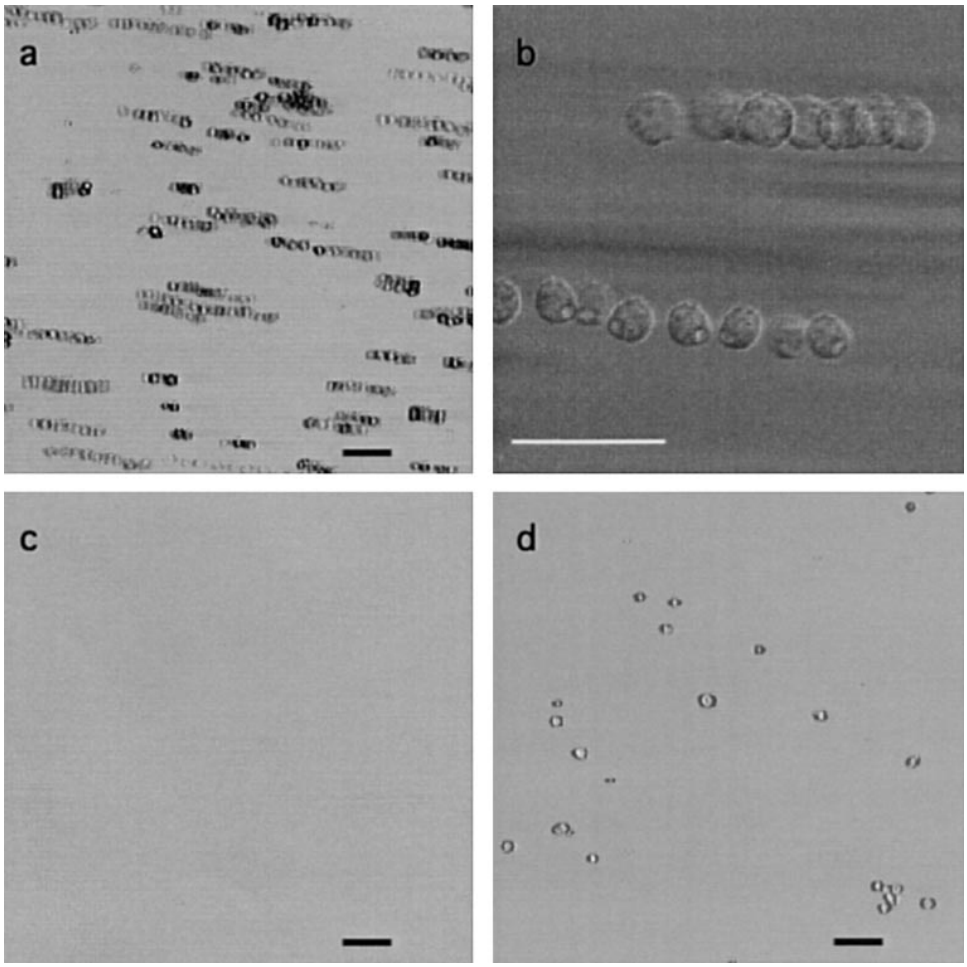

Figure 3. Stroboscopic images of free, attached, and rolling cells. 16 images spanning 6 s digitized from S-VHS tape (*a*, *c*, and *d*) or 8 images spanning 4 s directly acquired with a cooled CCD camera (40-ms exposure) (*b*) were added together such that the motion of cells in the flow field over time is represented in a single image. (*a*) I-GPI–transfected cells; (*b*) same as *a* at a higher magnification; (*c*) vector transfected cells; (*d*) ICAM-1 GPI-transfected cells. The bilayer membranes contained 500 molecules/μm^2 ICAM-1 (*a–c*) or 500 molecules/μm^2 LFA-1 (*d*). Scale bars = 50 μm.

I-GPI Cells Roll on ICAM-1– and ICAM-3–containing Bilayer Membranes. Laminar hydrodynamic flow produces a greater range of controlled shear stresses than can be applied by turbulent shear occurring in a 96-well plate adhesion assay. Therefore, adhesion of I-GPI E6 cells to a glass-supported planar bilayer reconstituted with 500 molecules/μm^2 purified ICAM-1 or 1,000 molecules/μm^2 purified ICAM-3 was examined in a parallel plate flow cell. The I-GPI E6 cells were allowed a 2-min static period to settle onto the bilayer before starting flow at a shear stress of 1 dyn/cm^2. Surprisingly, upon starting flow, the I-GPI E6 began to roll on planar bilayers containing ICAM-1 (Fig. 3, *A* and *B* and Table 1) or ICAM-3 (not shown), in a manner reminiscent of selectin- or VLA-4-mediated rolling. In contrast, mock

Table 1. *Qualitative and Quantitative Description of I Domain/ICAM-1 and ICAM-1/LFA-1 Adhesion in Flow*

			Pecent cells		
Cell type	Bilayer	Media	Free	Rolling	Stable
BHK pMON	ICAM-1	Mg^{2+}	100 ± 0	0	0
BHK ICAM-1	LFA-1	Mg^{2+}	73 ± 11	0	26 ± 9
BHK I-GPI E6	LFA-3	Mg^{2+}	98 ± 4	0	2 ± 4
BHK I-GPI E6	ICAM-1	Mg^{2+}	24 ± 15	72 ± 15	4 ± 4
BHK I-GPI E6	ICAM-1 + RR1/1	Mg^{2+}	100 ± 0	0	0

Cells were allowed to adhere statically for 2 min on bilayers containing 500 molecules/μm^2 each of ICAM-1, LFA-1, or LFA-3. Errors represent 95% confidence interval on the mean of free, rolling, or attached cells.

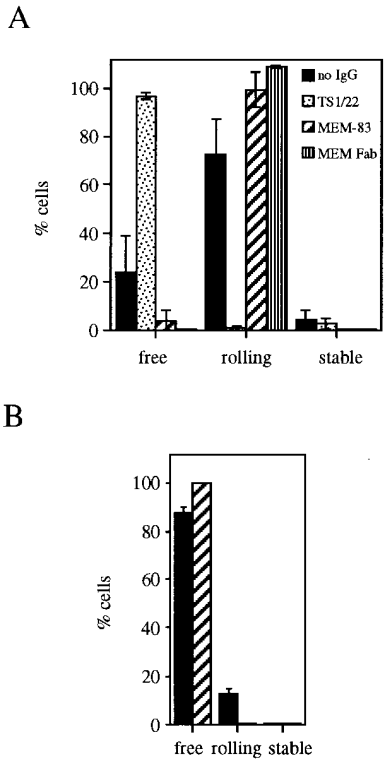

Figure 4. Effect of different anti–LFA-1 I domain antibodies on the interaction between I-GPI E6 cells and ICAM-1 (*A*) or ICAM-3 (*B*) containing bilayers at a flow rate of 1.1 dyn/cm^2. I-GPI E6 cells in HBS/BSA buffer containing 2 mM $MgCl_2$ were not treated (*black*) or pretreated with the antibodies TS1/22, MEM-83, or MEM-83 Fab fragments, and tested for rolling adhesion on bilayers at 500 ICAM-1 molecules/μm^2 (*A*) or bilayers at 1,000 ICAM-3 molecules/μm^2 (*B*). Error bars represent 95% confidence interval on the mean of free, rolling, or attached cells. $P < 0.03$ for rolling cells on ICAM-3.

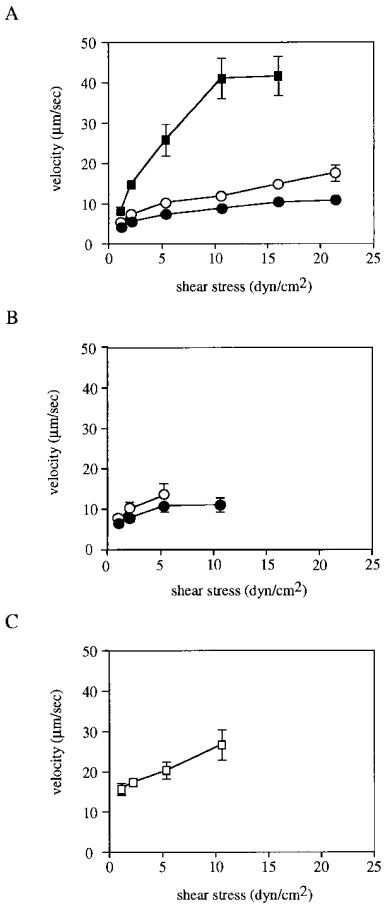

Figure 5. Rolling interaction of I-GPI cells with ICAM-1– (*A* and *B*) or ICAM-3– (*C*) containing bilayers. The rolling velocity of I-GPI E6 cells treated with no IgG (*solid square*), MEM-83 IgG (*solid circle*), or MEM-83 Fab (*open circle*) on membranes containing 500 molecules/μm^2 (*A*) or 150 molecules/μm^2 ICAM-1 (*B*) or 1,000 molecules/μm^2 ICAM-3 (*C*) as function of shear stress is shown. Error bars represent 95% confidence interval on the mean rolling velocity.

transfected cells showed neither rolling nor stable interaction with ICAM-1 in the glass-supported bilayer (Fig. 3 *C* and Table 1), whereas ICAM-1 GPI cells attached stably to bilayers containing 500 molecules/μm^2 of purified LFA-1 (Fig. 3 *D* and Table 1).

Effect of Antibodies on the Interaction between I-GPI E6 Cells and ICAM-1 or ICAM-3. Integrins are thought to undergo conformational changes, which can increase or decrease the affinity for ligands. This process can be induced by certain antibodies that bind the LFA-1 α or β subunit ectodomain. In this study, we investigated the influence of two monoclonal antibodies on the rolling interaction of I-GPI E6 cells with ICAMs in the flow cell. Both antibodies, TS1/22 and MEM-83, are known to bind to the I domain of the LFA-1 α subunit (6, 7, 10) (Fig. 1 *B*). While TS1/22 is a blocking antibody, MEM-83 increases lymphocyte adhesion to ICAM-1, but decreases lymphocyte adhesion to ICAM-3 (8, 10, 34).

Pretreatment of I-GPI E6 cells with the blocking antibody TS1/22 completly inhibited their rolling on ICAM-1–containing membranes (Fig. 4 *A*), indicating that the rolling interaction of I-GPI E6 cells on planar bilayers containing ICAM-1 is specific. As expected for a specific interaction, preincubation of the ICAM-1–containing bilayer membranes with the anti–ICAM-1 antibody RR1/1 also inhibited the rolling of I-GPI E6 cells (Table 1). Similarly, no attachment was seen between I-GPI cells and LFA-3–containing membranes (Table 1).

Pretreatment with the activating antibody MEM-83 IgG or Fab fragment increased the proportion of rolling cells on ICAM-1–containing membranes to 100% (Fig. 4 *A*). No increase in stable attachment was detected.

On ICAM-3 membranes (Fig. 4 *B*) in the presence of Mg^{2+}, fewer I-GPI E6 cells rolled ($\sim$13%) compared with ICAM-1. This is consistent with the idea of ICAM-3 being a less avid ligand for LFA-1 than ICAM-1. In these experiments, I-GPI E6 cells showed no stable attachment at all, and all interaction between I-GPI E6 cells and ICAM-3 was entirely of the rolling type. Therefore, we consider this percentage of rolling cells, although low, significant ($P < 0.03$). Pretreatment of I-GPI E6 cells with MEM-83 resulted in

complete abrogation of rolling on ICAM-3–containing membranes (Fig. 4 *B*). Taken together, these results suggest that MEM-83 is capable of inducing a conformational change in the I domain, leading to an increased avidity towards ICAM-1 and a decreased avidity towards ICAM-3. However, the MEM-83–induced increase in avidity of the I domain to ICAM-1 still results in a transient interaction that mediates rolling adhesion. Therefore, it is unlikely that the MEM-83 bound state is equivalent to the high affinity form of LFA-1. These results suggest that there is at least one other ligand binding site in the intact LFA-1 molecule.

The relative kinetics of the I-GPI/ICAM interaction were examined by measuring the rolling velocity of I-GPI E6 cells on ICAM-1– or ICAM-3–containing bilayers, respectively (Fig. 5). On bilayers containing 500 molecules/μm^2 of ICAM-1, an increasing shear stress resulted in a linear increase in the rolling velocity of I-GPI E6 cells in the presence of 2 mM Mg^{2+} that was paralleled by a decrease in the number of rolling cells (data not shown). The maximal average velocity was $\sim$40 μm/s at a shear stress of 12 dyn/cm^2 (Fig. 5 *A*). In the presence of MEM-83 or its Fab fragment, the rolling velocity of I-GPI E6 cells dropped considerably, especially at higher shear stresses, and reached maximal levels of $\sim$10 and $\sim$15 μm/s, respectively. To investigate whether the MEM-83–induced increase of avidity is sufficient to support rolling at low site densities, we reconstitued ICAM-1 into phosphatidylcholine at a site density of 150 ICAM-1 molecules/μm^2. In the absence of the activating antibody, very few I-GPI E6 cells rolled. In the presence of MEM-83 or MEM-83 Fab fragment, however, I-GPI E6 cells rolled on bilayers containing 150 molecules/μm^2 of ICAM-1 (Fig. 5 *B*). Altogether, it appears that MEM-83 increased the avidity of the I-GPI/ICAM-1 interaction about fourfold.

I-GPI E6 cells rolled on bilayers containing 1,000 molecules/μm^2 ICAM-3 (Fig. 5 *C*), but the rolling velocity did not level off at higher shear stresses, as with ICAM-1. However, stable attachment between the I domain and ICAMs was not observed under any condition. This suggests that the I domain/ICAM interaction is short lived and is in the range of other transient adhesion molecule interactions.

Role of Divalent Cations in the Transient Interaction of I-GPI with ICAM-1. The interaction between intact LFA-1 and ICAM-1 is dependent on the presence of Mg^{2+} ions (35). It can be enhanced by Mn^{2+} ions or by chelation of Ca^{2+} ions in the presence of Mg^{2+} (36). Full activation of LFA-1 is already achieved at low concentration of Mn^{2+} (>50 μM) (36), whereas higher concentrations of Mg^{2+} are required (35). Early studies with the I domain indicated cation independency (6), but in later studies (5, 10, 13, 15, 37) and crystallographic data (16–19) a requirement for either Mn^{2+} or Mg^{2+} ions has been shown. Therefore, it was of interest to investigate if I-GPI–mediated rolling in hydrodynamic flow was dependent on the presence of divalent cations.

In the presence of 2 mM Mg^{2+}, 72% of I-GPI E6 cells rolled on ICAM-1–containing bilayers at a flow rate of 1.1 dyn/cm^2 (Fig. 6 *A*). When Mg^{2+} was replaced by 0.2 mM Mn^{2+}, rolling of the I-GPI E6 cells was still supported. However, the percentage of rolling cells dropped to 16%, a fourfold reduction compared with Mg^{2+}. Rising the concentration of Mn^{2+} from 0.2 to 1 mM did not affect the percentage of rolling cells or the rolling velocity (data not shown). In the presence of 2 mM Ca^{2+}, no rolling was detectable (Fig. 6 *A*).

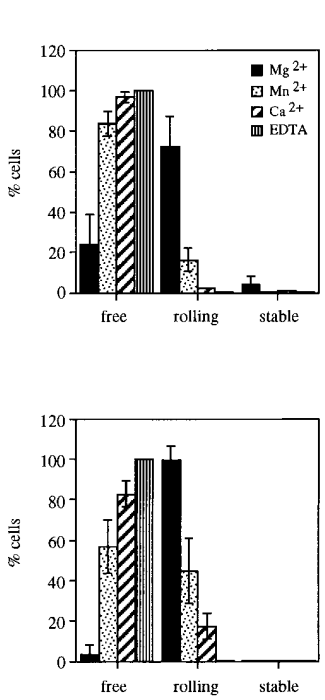

Figure 6. Ion dependency of the interaction of I-GPI E6 cells with ICAM-1–containing membranes in the absence (*A*) and presence (*B*) of MEM-83. I-GPI E6 cells in HBS/BSA buffer containing 2 mM $MgCl_2$ (*black*), 0.2 mM $MnCl_2$ (*stipled*), 1 mM $CaCl_2$ (*diagonal stripes*), or 2 mM EDTA (*vertical stripes*) were not treated (*A*) or pretreated with MEM-83 (0.1 mg/ml) (*B*), washed and assayed on bilayer membranes with 500 ICAM-1 molecules/μm^2 at a flow rate of 1.1 dyn/cm^2. Error bars represent 95% confidence interval on the mean of free, rolling, or attached cells.

If the I-GPI E6 cells were pretreated with the I domain activating antibody MEM-83, the percentage of rolling cells increased to 100% in the presence of Mg^{2+} and to 45% with Mn^{2+} (Fig. 6 *B*). Surprisingly, MEM-83–treated cells rolled on ICAM-1 bilayers in the presence of Ca^{2+} (Fig. 6 *B*). In this case, I-GPI E6 cells rolled to a lower extent than in the presence of Mg^{2+} or Mn^{2+} (data not shown). 2 mM EDTA always completely inhibited the interaction between I-GPI E6 cells and ICAM-1–containing bilayers (Fig. 6, *A* and *B*).

These data suggest a hierarchy of ion dependency in the I domain/ICAM-1 interaction with the order: $Mg^{2+} > Mn^{2+} > Ca^{2+}$. While Mn^{2+} can support some I-GPI/ICAM-1 interaction, the effect of Mn^{2+} seen here does not account for its dramatic influence on intact LFA-1 activity (36). Therefore, Mn^{2+} appears to act on another divalent cation binding site to enhance binding of intact LFA-1 to ICAM-1. These results suggest that the I-domain is not the only ligand binding site in LFA-1.

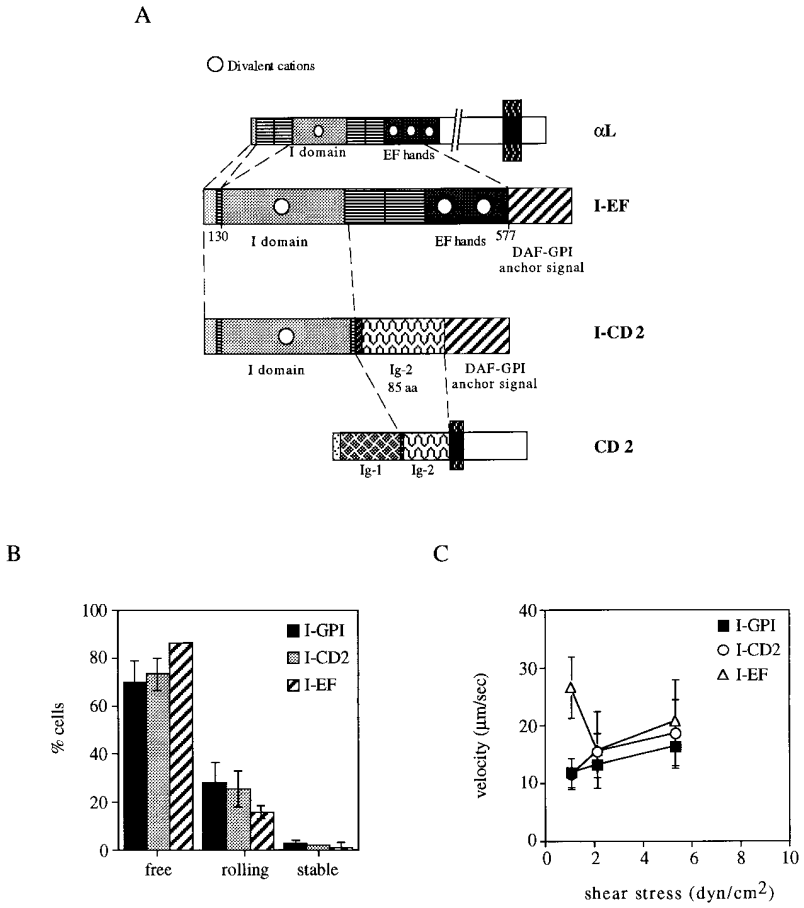

Figure 7. The distance of the I domain from the bilayer membrane does not result in a stable interaction. (*A*) Schematic of I-EF and I-CD2. In I-EF, the I domain was extended with repeats III, IV, V, VI, and the first few amino acids of repeat VII of the LFA-1 α chain. I-EF is linked to the Decay Accelerating Factor–GPI-anchoring signal as in I-GPI. In I-CD2, the spacer between the I domain and the Decay Accelerating Factor–GPI-anchoring signal consists of a few amino acids of the domain 1, the linker region, domain 2, and the stalk of human CD2. (*B*) Interaction of COS-1 cells transiently transfected with I-GPI, I-CD2, or I-EF, on membranes containing 500 molecules/μm^2 ICAM-1 in HBS/BSA containing 2 mM $MgCl_2$. The data were normalized according to a FACS® analysis and are presented as percent transfectants. The rolling interaction was statistically significant with $P < 0.01$ for each construct. (*C*) The rolling velocity of COS-1 cells transiently transfected with I-GPI, I-CD2, or I-EF on membranes containing 500 molecules/μm^2 ICAM-1 in HBS/BSA buffer containing 2 mM $MgCl_2$ was determined.

Rolling Interaction Does Not Depend on Close Spacing of the I Domain to the Plasma Membrane. Assuming that the I domain is situated in the globular head of the integrin detected in electron microscopic studies (38), the I domain in intact LFA-1 may protrude ~14 nm from the the plasma membrane. In I-GPI, this distance is only ~7 nm. The proximity to the plasma membrane might have a negative effect on the formation of stable bonds. To assess the effect of close spacing between the I domain and the plasma membrane on the rolling interaction, we designed two hybrid molecules, in which a spacer domain is inserted between the I domain and the GPI anchor. In one hybrid protein, the spacer consists of the stalk, the immunoglobulin superfamily (IgSF) domain 2, the linker, and 6 aa of the adjacent IgSF domain 1 of human CD2 (Fig. 7 *A*). According to the crystal structure of CD2 (39), the I domain should face upwards in this chimeric protein. In the other hybrid protein, the spacer comprised the repeats III, IV, V, VI, and 10aa of repeat VII of CD11a (Fig. 7 *A*). Repeats I–VII of the integrin α subunit were predicted to fold into a β-propeller domain with the I domain sitting on the upper face of it (40). The I-EF construct would only contain part of the β-propeller domain. The folding and the extensions of this construct and the relative position of the I domain therefore remain unclear. These chimeric proteins were termed I-CD2 and I-EF, respectively. I-CD2 and I-EF were transiently expressed on the surface of COS-1 cells (data not shown). As a control, I-GPI DNA was subcloned in the same expression vector and also transiently expressed in COS-1 cells. To determine the transfection levels of the different constructs, a FACS® analysis was performed in parallel to each flow cell experiment. The data from the flow cell experiments were normalized in respect to the expression levels of the various transfectants.

The fraction of I-CD2 and I-EF transfectants that were rolling on membranes containing 500 sites/μm^2 ICAM-1 was similar to that of I-GPI transfectants (Fig. 7 *B*). Overall, the number of transiently transfected COS-1 cells that were rolling on ICAM-1–containing bilayer membranes was considerably lower (~25%) than the number of rolling I-GPI E6 cells (~70%, Figs. 4 *A* and 6 *A*). This is probably due to the fact that the transiently transfected cells contain a whole spectrum of low to very high expressing cells. Since only cells expressing high levels of I domain can interact with ICAM-1 (Fig. 2), only a small fraction of I domain–expressing COS-1 cells is expected to show a rolling interaction on ICAM-1–containing bilayers. The rolling of I domain–expressing COS-1 cells is statistically significant with $P < 0.01$ in all cases. Similar to the fractions of rolling cells, the rolling velocities of I-CD2 and I-EF cells were

similar to that of I-GPI–expressing COS-1 cells (Fig. 7 *C*). The rolling velocities of ~10 μm/s at shear stresses of 1.1 and 2.1 dyn/cm^2 were also comparable with those seen for I-GPI E6 cells (Fig. 5 *A*). In contrast to the smooth rolling of the stably transfected I-GPI E6 cells, the rolling of the transiently transfected COS-1 cells was jerky, probably due to the more irregular shape of COS-1 cells.

In summary, we conclude from these experiments that the rolling interaction between the I-GPI and ICAM-1 is not caused by the short spacing of the I domain from the membrane. Rather, the transient, strain-resistant rolling interaction with ICAMs is an intrinsic property of the I domain.

Discussion

In the last few years, the I/A domain that is present in a subset of integrins has received intensive interest. This is partly due to the fact that the I/A domain contains a conserved ligand binding motive that adopts a Rossman fold and includes a novel metal-ion binding site (16). It was therefore tempting to examine the interaction between the I domain and their ligands in the context of integrin-mediated adhesion. Using a membrane-anchored form of the CD11a I domain and a parallel plate flow cell assay, we have shown in this study that the I domain is a transient binding module for the ligands ICAM-1 and ICAM-3, which is dependent on the presence of divalent cations, especially Mg^{2+}. Therefore, we propose that another binding site exists in LFA-1, which can be exposed through Mn^{2+} binding. These two binding modules cooperate to give rise to the high affinity stable binding seen in the intact LFA-1.

The binding affinity of purified Mac-1 (CD11b) A domain and its ligands iC3b and fibrinogen has been determined to be 300 ± 113 (37) and 220 ± 60 nM (14), respectively. Thus, the K_d value of the Mac-1 A domain to C3bi was ~30-fold higher than that of purified intact Mac-1 (12.5 ± 4.7 nM) (37). To date, no estimates are available for the affinity of the LFA-1 I domain. Here, we determined that sICAM-1 interacts with the LFA-1 I domain with a low affinity (K_d 100–200 μM) by competitively inhibiting the binding of radiolabeled Fab fragments with sICAM-1, a method that has been used previously to determine low affinity interactions (33). In agreement with our results, a study in the mouse system provided evidence for a high K_d of the interaction between LFA-1 on unstimulated T cells and ICAM-1 (~100 μM) (33). Altogether, the lower binding affinity of the intact LFA-1 towards ICAM-1 compared with that of Mac-1 towards C3bi also pertains to their I/A domains, respectively. Interactions with such high K_d values can be measured only with great difficulty. Therefore, we decided to study the I domain in adhesive interactions involving numerous bonds simultaneously rather than measuring single interactions.

To achieve this, we used a GPI-anchored form of the I domain (I-GPI). Thus, postreceptor events like cytoskeletal association and signal-induced affinity changes are excluded here. Such events were estimated to boost the rate and the efficiency of adhesion approximately four- to fivefold in the interaction between fibronectin and its ligand (41). Thus, we would expect that adhesion of I-GPI cells to ICAM-1 is in the range of the adhesion of unstimulated SKW3 cells to ICAM-1 bilayers or lower. We confirmed these assumptions in a static adhesion assay demonstrating that a 10-fold higher site density of I-GPI molecules is necessary to give a level of adhesion similar to that of unstimulated SKW3 cells. Therefore, we consider the interaction between the I domain–expressing cells and ICAM-1 bilayers of low avidity.

To overcome the caveats of static adhesion assays, we employed a parallel plate flow system, which allowed tight control of the shear stress and could be used in a quantitative manner to study the low avidity interaction of the I domain and ICAMs. The result was surprising: the I-GPI E6 cells showed a rolling interaction with their ligands (Fig. 3) over a large range of applied shear stresses. Rolling is a specific characteristic reported in only a few systems. Recently, this property has been described for the interaction of the α4 integrins with their ligands MadCAM-1 and VCAM-1 (42). In contrast with those integrins, which can support rolling and arrest after activation, the I domain supported rolling only, even in the presence of the activating antibody MEM-83. In this respect, the I domain behaved more like a selectin than an α4 integrin. Unlike the selectins and the α4 integrins, however, the I domain is unable to initiate tethering out of flow, in the range of shear stresses used here. In this respect, the I domain interaction with ICAM-1 and ICAM-3 is unique. Rolling adhesion implies a relatively fast off rate, the failure to accumulate a large number of bonds in the contact area, and bonds that can withstand longitudinal forces in the range of 100 pN without instantaneously rupturing (20). Therefore, the I domain/ICAM interaction has to be strain resistant to the extent that a small number of bonds can tether the rolling cell long enough for new bonds to form.

The rolling adhesion is a specific property of the I-GPI/ICAM-1 interaction and was not caused by extraction of the GPI-anchored proteins from the BHK cell membrane under our conditions, since the rolling velocity could be reduced upon pretreatment of the I-GPI E6 cells with Fab fragments of the activating antibody MEM-83 (Fig. 5, *A* and *B*). Furthermore, I-GPI cells sheared from ICAM-1 substrates did not undergo any decrease in surface expression of I-GPI, as would be the case when the I-GPI anchor is pulled out of the cell membrane (data not shown).

In the intact LFA-1 molecule, the I domain is placed at a certain distance from the plasma membrane. Recently Patel al. (43) reported that the number and rolling velocity of neutrophils interacting with chimeric P-selectin correlated inversely with the length of the chimeric P-selectin under flow conditions. The authors concluded that the distance of P-selectin from the plasma membrane may facilitate receptor–ligand interaction by protruding above the glycocalix and thereby decreasing the cell–cell repulsion. In another study, an extension of CD2 with the Ig-like domains

of ICAM-1 only resulted in more efficient binding to LFA-3 at a lower temperature, but had no effect at 24 or 37°C (44). To test if extending the spacing between the I domain and the plasma membrane would result in reduced rolling velocity, or even stable adhesion to ICAM-1, we inserted two different spacer domains between the I domain and the GPI anchoring signal (Fig. 7 *A*). According to the crystal structure of CD2, the I domain is expected to protrude upwards in the chimeric protein. The linker region of CD2 allows extension and conformational flexibility of the I domain (39). The length of this spacer is ~4 nm (39). Together with the ~3-nm extension provided by the GPI anchoring signal (45) and the ~4 nm of the I domain, the I-CD2 fusion protein has an overall length of 11 nm, which is in the range of L-selectin, but shorter than the cutoff for interaction with P-selectin (16 nm; reference 43). ICAM-1 is ~19 nm long and the thickness of the glycocalyx is estimated to be between 5 and 20 nm. In flow cell experiments with reconstituted bilayer membranes, which lack a glycocalyx, only the glycocalyx of the interacting cells needs to be bridged. For this reason, electrostatic cell membrane repulsion should not play a role in our system. The length of the I-CD2 molecule should therefore be sufficient to allow an interaction with ICAM-1 unperturbed by the glycocalyx.

In this study, we used the monoclonal antibodies TS1/22 and MEM-83 to characterize the I domain interaction with ICAM-1 and ICAM-3. While TS1/22 is a blocking antibody (7) and prevented rolling of I-GPI E6 cells on ICAM-1 bilayers (Fig. 4 *A*), MEM-83 has been described as an activating antibody towards ICAM-1 and as a blocking antibody towards ICAM-3 (8, 10, 12, 34). This was also reflected in our experiments, in which preincubation with MEM-83 increased the number of rolling I-GPI E6 cells and decreased the rolling velocity on ICAM-1 bilayer membranes (Figs. 4 *A* and 5, *A* and *B*), while it inhibited rolling on ICAM-3 bilayers (Fig. 4 *B*).

Recently, the crystal structures of the Mac-1 (16, 17) and the LFA-1 (18, 19) I domains have been published. The Mac-1 I domain was crystallized in two forms: one in the presence of Mg^{2+} (16), the other in the presence of Mn^{2+} (17). Based on these data, it has been suggested that the I domain is the only ligand binding site in Mac-1, and the Mg^{2+} bound form reflects the active (high affinity) state, whereas the Mn^{2+} bound form represents the low affinity state. The LFA-1 I domain was initially crystallized in the presence of Mn^{2+} (18), later the crystal structure in the presence of Mg^{2+} and EDTA became available (19). In contrast to the Mac-1 I domain, the LFA-1 I domain does not show dramatic conformational differences in the presence of Mg^{2+} or Mn^{2+}. These results are consistent with our finding that both Mg^{2+} and Mn^{2+} supported rolling of I-GPI cells on ICAM-1 bilayers. However, both ions differed in their efficiency and none was able to induce the stable adhesion on ICAM-1 bilayers, which is a hallmark of the intact LFA-1 molecule. Furthermore, Mn^{2+} appears to be the more potent activator of the intact LFA-1 molecule than Mg^{2+} (36, 46), which is not reflected in the hierarchy of cation-dependent rolling detected here with the I domain. Therefore, we propose that Mn^{2+} acts on another site in LFA-1, different from the I domain, which cooperates with the I domain to give rise to the stable interaction of intact LFA-1 with ICAM-1 and ICAM-3.

Several studies looked for potential ligand binding sites outside the I domain (4, 5, 47). Apart from the I domain, the EF-hand repeats V and VI of the LFA-1 α-subunit were implicated in ligand binding (4). Alanine substitutions in putative metal-ion–dependent adhesion sites in the β_2-subunit (5, 47) resulted in loss of adhesion to ICAM-1 and fibrinogen. So far, it is not known if these sites are also transient binding modules and if they act in a cooperative or sequential manner. However, the use of multiple modules, with at least one of them transient and strain resistant, to build a single high affinity binding surface would be an elegant concept for integrins, which are required to rapidly interconvert from low to high affinity forms and vice versa.

We thank Drs. E. Unanue and S. Teitelbaum for their support. We also thank J. Miller and R. Houdei for technical assistance and Drs. D. Lublin, D. Griggs, V. Horesij, T. Springer, and D. Staunton for providing important reagents. Drs. R. Lindner, R. Brown, S. Santoro, C. Lu, T. Springer, D. Hammer, and L. Dustin are thanked for helpful comments and discussions.

This work was supported in part by the Monsanto-Searle/Washington University Biomedical Research Agreement.

Address correspondence to Dr. Ruth Knorr or Dr. Michael L. Dustin, Center for Immunology and Department of Pathology, Box 8118, Washington University School of Medicine, 660 S. Euclid Avenue, St. Louis, MO 63110.

Received for publication 9 May 1997 and in revised form 1 July 1997.

References

1. Dustin, M.L., and T.A. Springer. 1991. Role of lymphocyte adhesion receptors in transient interactions and cell locomotion. *Annu. Rev. Immunol.* 9:27–66.
2. Lub, M., Y. van Kooyk, and C.G. Figdor. 1995. Ins and outs of LFA-1. *Immunol. Today*. 16:479–483.
3. Stewart, M.P., and N. Hogg. 1996. Regulation of leukocyte

integrin function: affinity vs. avidity. *J. Cell. Biochem.* 61:554–561.

4. Stanley, P., P.A. Bates, J. Harvey, R.I. Bennett, and N. Hogg. 1994. Integrin LFA-1 α subunit contains an ICAM-1 binding site in domains V and VI. *EMBO (Eur. Mol. Biol. Organ.) J.* 13:1790–1798.
5. Goodman, T.G., and M.L. Bajt. 1996. Identifying the putative metal ion-dependent adhesion site in the β_2 (CD18) subunit required for $\alpha_L\beta_2$ and $\alpha_M\beta_2$ ligand interactions. *J. Biol. Chem.* 271:23729–23736.
6. Randi, A.M., and N. Hogg. 1994. I domain of β_2 integrin lymphocyte function-associated antigen-1 contains a binding site for ligand intercellular adhesion molecule-1. *J. Biol. Chem.* 269:12395–12398.
7. Huang, C., and T.A. Springer. 1995. A binding interface on the I domain of lymphocyte function-associated antigen-1 (LFA-1) required for specific interaction with intercellular adhesion molecule-1 (ICAM-1). *J. Biol. Chem.* 270:19008–19016.
8. van Kooyk, Y., M.E. Binnerts, C.P. Edwards, M. Champe, P.W. Berman, C.G. Figdor, and S.C. Bodary. 1996. Critical amino acids in the lymphocyte function-associated antigen-1 I domain mediate intercellular adhesion molecule 3 binding and immune function. *J. Exp. Med.* 183:1247–1252.
9. Kamata, T., R. Wright, and Y. Takada. 1995. Critical threonine and aspartic acid residues within the I domains of β_2 integrins for interactions with intercellular adhesion molecule 1 (ICAM-1) and C3bi. *J. Biol. Chem.* 270:12531–12535.
10. Edwards, C.P., M. Champe, T. Gonzalez, M.W. Wessinger, S.A. Spencer, L.G. Presta, P.W. Berman, and S.C. Bodary. 1995. Identification of amino acids in the CD11a I-domain important for binding of the leukocyte function-associated antigen-1 (LFA-1) to intercellular adhesion molecule-1 (ICAM-1). *J. Biol. Chem.* 270:12635–12640.
11. Diamond, M.S., J. Garcia-Aguilar, J.K. Bickford, A.L. Corbi, and T.A. Springer. 1993. The I domain is a major recognition site on the leukocyte integrin Mac-1 (CD11b/CD18) for four distinct adhesion ligands. *J. Cell Biol.* 120:1031–1043.
12. Landis, R.C., R.I. Bennett, and N. Hogg. 1993. A novel LFA-1 activation epitope maps to the I-domain. *J. Cell Biol.* 120:1519–1527.
13. Ueda, T., P. Rieu, J. Brayer, and M.A. Arnaout. 1994. Identification of the complement iC3b binding site in the β_2 integrin CR3 (CD11b/CD18). *Proc. Natl. Acad. Sci. USA.* 91: 10680–10684.
14. Zhou, L., D.H.S. Lee, J. Plescia, C.Y. Lau, and D.C. Altieri. 1994. Differential ligand binding specificities of recombinant CD11b/CD18 integrin I-domain. *J. Biol. Chem.* 269:17075–17079.
15. Kern, A., R. Breisewitz, I. Bank, and E.E. Marcantonio. 1994. The Role of the I domain in ligand binding of the human integrin $\alpha_1\beta_1$. *J. Biol. Chem.* 269:22811–22816.
16. Lee, J.O., P. Rieu, M.A. Arnaout, and R. Liddington. 1995. Crystal structure of the A domain from the α subunit of integrin CR3 (CD11b/CD18). *Cell.* 80:631–638.
17. Lee, J.O., L.A. Bankston, M.A. Arnaout, and R.C. Liddington. 1995. Two conformations of the integrin A-domain (I-domain) a pathway for activation? *Structure (Lond.).* 3:1333–1340.
18. Qu, A., and D.J. Leahy. 1995. Crystal structure of the I-domain from the CD11a/CD18 (LFA-1, $\alpha_L\beta_2$) integrin. *Proc. Natl. Acad. Sci. USA.* 92:10277–10281.
19. Qu, A., and D.J. Leahy. 1996. The role of the divalent cation in the structure of the I domain from the CD11a/CD18 integrin. *Structure (Lond.).* 4:931–942.
20. Alon, R., D.A. Hammer, and T.A. Springer. 1995. Lifetime of the P-selectin:carbohydrate bond and its response to tensile force in hydrodynamic flow. *Nature (Lond.).* 374:539–542.
21. Pierres, A., A.M. Benoliel, P. Bongrand, and P.A. van der Merwe. 1996. Determination of the lifetime and force dependence of interactions of single bonds between surface-attached CD2 and CD48 adhesion molecules. *Proc. Natl. Acad. Sci. USA.* 93:15114–15118.
22. Warren, T.G., P.J. Hippenmeyer, D.M. Meyer, B.A. Reitz, E. Rowold, and C.P. Carron. 1994. High-level expression of biologically active, soluble forms of ICAM-1 in a novel mammalian-cell expression system. *Protein Expr. Purif.* 5:498–508.
23. Coyne, K.E., A. Crisci, and D.M. Lublin. 1993. Construction of synthetic signals for glycosyl-phosphatidylinositol anchor attachment. Analysis of amino acid sequence requirements for anchoring. *J. Biol. Chem.* 268:6689–6693.
24. Horton, R.M., H.D. Hunt, S.N. Ho, J.K. Pullen, and L.R. Pease. 1989. Engineering hybrid genes without the use of restriction enzymes: gene splicing by overlap extension. *Gene.* 77:61–68.
25. Seed, B., and A. Aruffo. 1987. Molecular cloning of the CD2 antigen, the T-cell erythrocyte receptor, by a rapid immunoselection procedure. *Proc. Natl. Acad. Sci. USA.* 84:3365–3369.
26. Parham, P., M.J. Androlewicz, F.M. Brodsky, N.J. Holmes, and J.P. Ways. 1982. Monoclonal antibodies: purification, fragmentation and application to structural and functional studies of class I MHC antigens. *J. Immunol. Methods.* 53:133–173.
27. Kucik, D.F., M.L. Dustin, J.M. Miller, and E.J. Brown. 1996. Adhesion activating phorbol ester increases the mobility of leukocyte integrin LFA-1 in cultured lymphocytes. *J. Clin. Invest.* 97:2139–2144.
28. Mimms, L.T., G. Zampighi, Y. Nozaki, C. Tanford, and J.A. Reynolds. 1981. Phosholipid vesicle formation and transmembrane protein incorporation using octyl glucoside. *Biochemistry.* 20:833–840.
29. Cheng, Y.C., and W.H. Prusoff. 1973. Relationship between the inhibition constant (Ki) and the concentration of inhibitor which causes 50 per cent inhibition (I50) of an enzymatic reaction. *Biochem. Pharm.* 22:3099–3108.
30. Dustin, M.L., and T.A. Springer. 1989. T cell receptor cross-linking transiently stimulates adhesiveness through LFA-1. *Nature (Lond.).* 341:619–624.
31. McConnell, H.M., T.H. Watts, R.M. Weis, and A.A. Brian. 1986. Supported planar membranes in studies of cell–cell recognition in the immune system. *Biochim. Biophys. Acta.* 864: 95–106.
32. Low, M.G., and J. Bryan Finean. 1978. Specific release of membrane enzymes by a phosphotidylinositol-specific phospholipase C. *Biochim. Biophys. Acta.* 508:565–570.
33. Lollo, B.A., K.W.H. Chan, E.M. Hanson, V.T. Moy, and A.A. Brian. 1993. Direct evidence for two affinity states for lymphocyte function-associated antigen-1 on activated T cells. *J. Biol. Chem.* 268:21693–21700.
34. Binnerts, M.E., Y. van Kooyk, D.L. Simmons, and C.G. Figdor. 1994. Distinct binding of T lymphocytes to ICAM-1, -2 or -3 upon activation of LFA-1. *Eur. J. Immunol.* 24:2155–2160.
35. Rothlein, R., and T.A. Springer. 1986. The requirement for

lymphocyte function-associated antigen 1 in homotypic leukocyte adhesion stimulated by phorbol ester. *J. Exp. Med.* 163:1132–1149.
36. Dransfield, I., C. Cabanas, A. Craig, and N. Hogg. 1992. Divalent cation regulation of the function of leukocyte integrin LFA-1. *J. Cell Biol.* 116:219–226.
37. Cai, T.Q., S.K.A. Law, H.R. Zhao, and S.D. Wright. 1995. Reversible inactivation of purified leukocyte integrin CR3 (CD11b/CD18, $\alpha_M\beta_2$) by removal of divalent cations from a cryptic site. *Cell Adhes. Commun.* 3:399–406.
38. Nermut, M.V., N.M. Green, P. Eason, S.S. Yamada, and K.M. Yamada. 1988. Electron microscopy and structural model of human fibronectin receptor. *EMBO (Eur. Mol. Biol. Organ.) J.* 7:4093–4099.
39. Davis, S.J., and P.A. van der Merwe. 1996. The structure and ligand interactions of CD2: implications for T-cell function. *Immunol. Today.* 17:177–187.
40. Springer, T.A. 1997. Folding of the N-terminal, ligand-binding region of the integrin α-subunits into a β-propeller domain. *J. Biol. Chem.* 94:65–72.
41. Danilov, Y.N., and R.L. Juliano. 1989. Phorbol ester modulation of integrin-mediated cell adhesion: a postreceptor event. *J. Cell Biol.* 108:1925–1933.
42. Berlin, C., R.F. Bargatze,. J. Campbell, U.H. von Andrian,. C. Szabo, S.R. Hasslen, R.D. Nelson, E.L. Berg, S.L. Erlandsen, and E.C. Butcher. 1995. α4 integrins mediate lymphocyte attachment and rolling under physiological flow. *Cell.* 80:413–422.
43. Patel, K.D., M.U. Nollert, and R.P. McEver. 1995. P-selectin must extend a sufficient length from the plasma membrane to mediate rolling of neutrophils. *J. Cell Biol.* 131: 1893–1902.
44. Chan, P.Y., and T.A. Springer. 1992. Effect of lengthening lymphocyte function-associate 3 on adhesion to CD2. *Mol. Biol. Cell.* 3:157–166.
45. Perkins, S.J., A.F. Williams, T.W. Rademacher, and R.A. Dwek. 1988. The Thy-1 glycoprotein: a three-dimensional model. *TIBS (Trends Biochem. Sci.).* 13:302–303.
46. Gailit, J., and E. Ruoslahti. 1988. Regulation of the fibronectin receptor affinity by divalent cations. *J. Biol. Chem.* 263: 12927–12932.
47. Tozer, E.C., R.C. Liddington, M.J. Sutcliffe, A.H. Smeeton, and J.C. Loftus. 1996. Ligand binding to integrin $\alpha_{IIb}\beta_3$ is dependent on a MIDAS-like domain in the β_3 subunit. *J. Biol. Chem.* 271:21978–21984.